AIAA JOURNAL
Vol. 46, No. 11, November 2008

Robust Eigenvalue Analysis Using the Structured Singular Value: The μ-p Flutter Method

Dan Borglund*
Royal Institute of Technology, 100 44 Stockholm, Sweden

DOI: 10.2514/1.35859

This paper introduces a new technique for robust aeroelastic analysis that extends standard linear flutter analysis to take deterministic uncertainty and variation into account. The basic principle of the proposed μ-p method is to exploit structured-singular-value (or μ) analysis to investigate if the system uncertainties can make the flutter determinant zero for a given flutter eigenvalue p. This makes it possible to compute regions of feasible eigenvalues in the complex plane as well as extreme eigenvalues that can be used to predict damping bounds and perform robust flutter analysis. The capability to predict damping bounds at subcritical flight conditions is a very attractive feature of the new method, as flight testing is rarely taken to the flutter point. The μ-p formulation also opens up new possibilities to bound the magnitude of the system uncertainties based on frequency and/or damping estimates from flight testing. In the final part of the paper, the μ-p framework is successfully applied to perform robust aeroelastic analysis of a low-speed wind-tunnel model.

Nomenclature

F	=	flutter matrix
$\mathcal{F}_u$	=	upper linear fractional transformation
g	=	damping
K	=	stiffness matrix
k	=	reduced frequency
L	=	reference length
M	=	mass matrix
N	=	linear fractional transformation matrix
P	=	system matrix
p	=	eigenvalue
Q	=	aerodynamic matrix
V	=	airspeed
w	=	input from uncertainty matrix
z	=	output to uncertainty matrix
Δ	=	uncertainty matrix
δ	=	uncertainty parameters
η	=	modal coordinates
μ	=	structured singular value
ξ	=	modal force
ρ	=	air density
$\bar{\sigma}$	=	maximum singular value

Introduction

FLIGHT flutter testing is always associated with high risk, because it can potentially lead to structural damage or failure. A reliable flutter analysis is therefore a vital component of any test campaign, because it enables more confident decisions through a successive comparison of predictions and test results. However, the development of a reliable flutter analysis still poses a great challenge to aeroelasticians, because the complex character of aeroelastic phenomena gives rise to many different sources of error and uncertainty.

A fairly recent approach to deal with deterministic uncertainty and variation of aeroelastic models was initiated by Lind and Brenner [1] and Lind [2], who first demonstrated the use of so-called μ analysis [3] to perform robust flutter analysis. Later, Borglund [4,5] and Borglund and Ringertz [6] developed the μ-k method, which is based on traditional frequency-domain flutter analysis. As a result, the robust analysis can be performed using existing numerical models and inherently produces match-point flutter solutions. The μ-k formulation also opened up new possibilities to model aerodynamic uncertainty, which is of primary importance in aeroelastic applications. Some additional developments in this direction can be found in [7–10].

Although significant progress has been made, the current methods for robust flutter analysis suffer from an apparent shortcoming. So far, the main objective of the robust analysis has been to compute a worst-case flutter speed subject to a given uncertainty description. Although a worst-case flutter speed is certainly an important result, its usefulness when it comes to flight flutter testing is limited. The reason for this is that the flight testing is rarely taken to the flutter point. It is rather desirable to clear the flight envelope without reaching a flutter condition at all. The practical usefulness of such a method would therefore increase substantially if it could be used to perform robust analysis of properties that can be estimated at subcritical flight conditions, such as the damping of a particular mode.

In this paper, the μ-k method is generalized to the Laplace domain to allow for robust analysis at any flight condition. The net result is a new μ-p method that extends standard linear flutter analysis to take deterministic uncertainty and variation into account. Where a standard flutter solver [11,12] computes a set of flutter eigenvalues in the complex plane, the μ-p method computes regions of feasible eigenvalues in the complex plane. From these regions, the possible variation of frequency and damping of different aeroelastic modes can be determined. This capability can either be used to perform robust analysis for a validated uncertainty description or to perform sensitivity analysis. The μ-p framework also provides new means for model validation in which frequency and damping data from flight testing can be used to estimate the level of uncertainty present in the model.

Uncertain Flutter Equation

The concept of robust flutter analysis can be introduced by considering the Laplace-domain equations of motion with uncertainty and/or variation:

$$F(p,\delta)\eta = [M(\delta)p^2 + (L^2/V^2)K(\delta) - (\rho L^2/2)Q(p,\delta)]\eta = 0 \tag{1}$$

Received 26 November 2007; accepted for publication 30 June 2008.

*Research Associate, Department of Aeronautical and Vehicle Engineering, Division of Flight Dynamics, Teknikringen 8. Member AIAA.

where $M(\delta)$ is the mass matrix, $K(\delta)$ is the stiffness matrix, $Q(p, \delta)$ is the aerodynamic transfer matrix, η is the vector of modal coordinates, V is the airspeed, L is the aerodynamic reference length, and ρ is the air density. The nondimensional Laplace variable is denoted as $p = g + ik$, where g is the damping and k is the reduced frequency. Note that the dependence on the Mach number and structural damping have been omitted for conciseness.

Although the μ framework from the control community allows for various types of uncertainties [3], this work uses a parametric uncertainty model to introduce and demonstrate the basic principle of μ-p flutter analysis. Parametric uncertainty descriptions can be used to represent many different uncertainty mechanisms in aeroelastic systems and can often be derived using physical insight and reasoning. The mass, stiffness, and aerodynamic matrices are assumed to depend on a set of unknown but bounded parameters in the vector δ. For convenience, it is further assumed that the uncertainty parameters have been normalized such that $|\delta_j| \leq 1$ holds for each parameter and that $\delta = 0$ corresponds to the nominal model without uncertainty. This means that $\delta \in D$, where the set $D = \{\delta : \|\delta\|_\infty \leq 1\}$. Note that both real and complex parameters are possible, typically representing mass/stiffness and aerodynamic uncertainty, respectively.

The uncertain flutter equation (1) is a nonlinear eigenvalue problem that defines a set of eigenvalues $p(\delta)$ and eigenvectors $\eta(\delta)$ for each $\delta \in D$. In particular, the eigenvalues are the values of p making the flutter matrix $F(p, \delta)$ singular, such that $\det[F(p, \delta)] = 0$ holds. Depending on the formulation used for the aerodynamic forces, the eigenvalue problem can (for a given δ) be solved using, for example, the p-k method [11] or the g method [12]. Although the system is nominally stable if all nominal eigenvalues $p_0 = p(0)$ have negative real parts, robust stability requires that all eigenvalues $p(\delta)$ have negative real parts for all $\delta \in D$. In the same manner, the system is robustly unstable if some $p(\delta)$ has a positive real part for all $\delta \in D$.

As the eigenvalues are continuous functions of the matrix elements in the flutter equation (see [13]), each nominal eigenvalue will expand to a set of feasible eigenvalues in the complex plane for $\delta \in D$. This is illustrated for one distinct eigenvalue in Fig. 1. Apparently, the corresponding mode is robustly stable if the eigenvalue set is restricted to the left half-plane. The robust flutter boundary is reached when the eigenvalue set crosses the imaginary axis at $\mathrm{Re}(p) = 0$, because some $\delta \in D$ can then destabilize the mode. Of particular interest are the eigenvalues p_- and p_+, with the minimum and maximum real parts, respectively. These eigenvalues provide damping bounds for the mode, and if p_+ has a negative real part, the mode is robustly stable.

It would be very desirable to be able to compute the boundary of the eigenvalue set in the complex plane as well as the extreme eigenvalues p_- and p_+. In simple cases, it may be possible to characterize the eigenvalue set by performing a systematic sweep of the parameter space [6], but this method becomes computationally infeasible, even for a modest number of parameters. It is also possible to pose an explicit optimization problem to minimize or maximize the real part of an eigenvalue using the uncertainty parameters as variables [14,15]. Here, the main obstacle is that the optimization problem is, in general, nonconvex and so robustness cannot be guaranteed. These approaches also lack a structured framework and tend to become very dependent on the specific problem. The next section will introduce the μ-p method, which uses the linear fractional transformation (LFT) framework [16] and μ analysis [3] to accomplish the desired objectives.

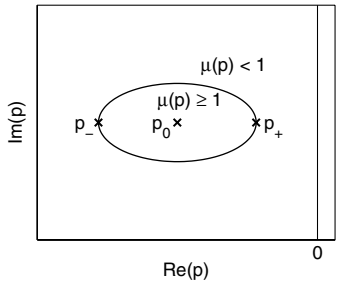

Fig. 1 Set of feasible eigenvalues in the complex plane.

Flutter Analysis Using the μ-p Method

The basic principle of the μ-p method is to exploit μ analysis to investigate if some uncertainty $\delta \in D$ can make the flutter determinant $\det[F(p, \delta)] = 0$ for a given value of p. If this is true, then p is an eigenvalue of the uncertain flutter equation (1) for some $\delta \in D$. The first step is to pose the flutter equation in a form that is suitable for μ analysis. This can be accomplished using simple LFT matrix operations [16], as described in the following sections.

LFT Formulation

By deriving individual LFTs for the different terms in Eq. (1), it is possible to write the uncertain flutter equation in the assembled LFT form:

$$F(p, \delta)\eta = \mathcal{F}_u(N(p), \Delta)\eta = [N_{22} + N_{21}\Delta(I - N_{11}\Delta)^{-1}N_{12}]\eta = 0 \tag{2}$$

where $\mathcal{F}_u(N(p), \Delta)$ is an upper LFT representation of the uncertain transfer matrix $F(p, \delta)$ between the modal coordinates η and force ξ, as shown in Fig. 2a. The uncertainty parameters $\delta \in D$ are now isolated to a block-structured uncertainty matrix Δ that belongs to a corresponding set B defined as

$$B = \{\Delta : \Delta \text{ structured and } \bar{\sigma}(\Delta) \leq 1\} \tag{3}$$

where $\bar{\sigma}(\cdot)$ denotes the maximum singular value (the induced 2-norm). The LFT matrix $N(p)$ is partitioned with respect to the input and output signals according to

$$N(p) = \begin{bmatrix} N_{11}(p) & N_{12}(p) \\ N_{21}(p) & N_{22}(p) \end{bmatrix} \tag{4}$$

where the different partitions depend on the nominal elements of the flutter equation and scaling matrices originating from the uncertainty description. By inserting $\Delta = 0$ (corresponding to $\delta = 0$) in Eq. (2), it can, for example, be noted that $N_{22}(p)$ is equal to the nominal flutter matrix:

$$N_{22}(p) = F_0(p) = M_0 p^2 + (L^2/V^2)K_0 - (\rho L^2/2)Q_0(p) \tag{5}$$

In the basic but important case of linear matrix perturbations, the flutter equation can be written in the form

$$[F_0(p) + F_1(p)\Delta F_2(p)]\eta = 0 \tag{6}$$

where $F_1(p)$ and $F_2(p)$ are scaling matrices that determine the magnitude and influence of the uncertainty [4,6]. In this case, it is trivial to identify the LFT matrix:

$$N(p) = \begin{bmatrix} 0 & F_2(p) \\ F_1(p) & F_0(p) \end{bmatrix} \tag{7}$$

where it can be noted that $N_{11}(p) = 0$. This means that the matrix $(I - N_{11}(p)\Delta)$ is nonsingular (hence invertible) and that the LFT in Eq. (2) is well defined [16]. This is expected for this application, because $\mathcal{F}_u(N(p), \Delta)$ is merely a different representation of the bounded transfer matrix $F(p, \delta)$. As described later, a μ criterion can be used to verify that $(I - N_{11}(p)\Delta)$ is nonsingular for structured Δ.

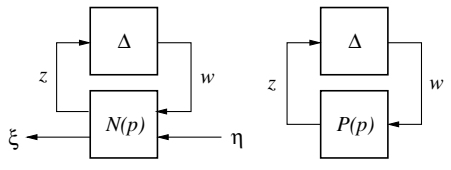

Fig. 2 Illustrations of a) LFT between η and ξ, b) feedback loop.

Equivalent Feedback Form

By enforcing $\xi = 0$ in the LFT in Fig. 2a, it is clear that Eq. (2) is a reduced form of the feedback equations:

$$w = \Delta z \tag{8}$$

$$z = N_{11} w + N_{12} \eta \tag{9}$$

$$0 = N_{21} w + N_{22} \eta \tag{10}$$

These equations can also be reduced to the equivalent feedback form,

$$[I - P(p)\Delta]z = 0 \tag{11}$$

which governs the dynamics of the feedback loop in Fig. 2b. In this form, the system matrix $P(p)$ is computed as the Schur complement [17] of $N_{22}(p)$ in $N(p)$,

$$P(p) = N_{11} - N_{12} N_{22}^{-1} N_{21} \tag{12}$$

which is well defined except at the nominal eigenvalues $p = p_0$ [where the nominal flutter matrix $N_{22}(p) = F_0(p)$ is singular]. In the case of linear matrix perturbations, represented by Eqs. (6) and (7), the system matrix becomes

$$P(p) = -F_2 F_0^{-1} F_1 \tag{13}$$

As shown by the following theorem, the equivalent-feedback-form equation (11) has the same eigenvalues as Eq. (2) if $(I - N_{11}(p)\Delta)$ and $N_{22}(p)$ are nonsingular.

Theorem. If $(I - N_{11}(p)\Delta)$ and $N_{22}(p)$ are nonsingular, then

$$\det(I - P(p)\Delta) = 0 \Leftrightarrow \det[F(p, \delta)] = 0 \tag{14}$$

Proof. First, assume that a set $\{p, \Delta, z\}$ solves the equivalent-feedback-form equation (11). Then the set

$$\{p, \Delta, z, w = \Delta z, \eta = -N_{22}^{-1} N_{21} \Delta z\}$$

solves Eqs. (8–10) and the set

$$\{p, \Delta, \eta = -N_{22}^{-1} N_{21} \Delta z\}$$

solves Eq. (2). This proves that

$$\det(I - P(p)\Delta) = 0 \Rightarrow \det[\mathcal{F}_u(N(p), \Delta)] = \det[F(p, \delta)] = 0$$

Next assume that a set $\{p, \Delta, \eta\}$ solves Eq. (2). Then the set

$$\{p, \Delta, z = (I - N_{11}\Delta)^{-1} N_{12} \eta, w = \Delta z, \eta\}$$

solves Eqs. (8–10) and the set

$$\{p, \Delta, z = (I - N_{11}\Delta)^{-1} N_{12} \eta\}$$

solves Eq. (11). Consequently,

$$\det[\mathcal{F}_u(N(p), \Delta)] = \det[F(p, \delta)] = 0 \Rightarrow \det(I - P(p)\Delta) = 0$$

This proves that if $(I - N_{11}(p)\Delta)$ and $N_{22}(p)$ are nonsingular for $\Delta \in B$ and some $\Delta \in B$ makes $\det(I - P(p)\Delta) = 0$, then p is an eigenvalue of the uncertain flutter equation (2) for some $\Delta \in B$ (or $\delta \in D$). Note that the nominal eigenvalues p_0 are a priori known to be eigenvalues of Eq. (2) for $\Delta = 0$ (or $\delta = 0$). The fact that $P(p)$ is not well defined at $p = p_0$ is therefore not a concern.

Robust Eigenvalue Analysis

It is now possible to apply structured-singular-value analysis to investigate the possible solutions to the uncertain flutter equation. For a given value of p, the structured singular value μ of the system matrix $P(p)$ is defined as the reciprocal of the minimum norm of any structured Δ, making $(I - P(p)\Delta)$ singular:

$$\mu[P(p)] = 1/\min_{\Delta}\{\bar{\sigma}(\Delta): \det(I - P(p)\Delta) = 0 \text{ for structured } \Delta\} \tag{15}$$

If no such structured Δ exists, then $\mu[P(p)] = 0$. Based on the results of the previous section, this means that if $(I - N_{11}(p)\Delta)$ and $N_{22}(p)$ are nonsingular for structured Δ and

$$\mu(p) \equiv \mu[P(p)] \geq 1 \tag{16}$$

then p is an eigenvalue of Eq. (2) for some $\Delta \in B$. Correspondingly, if $\mu(p) < 1$, then p is not an eigenvalue of Eq. (2) for $\Delta \in B$. This is a very powerful result, meaning that a single μ evaluation can be used to determine if a particular value of p is a solution to the uncertain flutter equation or not.

If it is not apparent that $(I - N_{11}(p)\Delta)$ is nonsingular for structured Δ [this holds if $N_{11}(p) = 0$, for example], the following criterion guarantees that $(I - N_{11}(p)\Delta)$ is nonsingular for the minimum norm Δ, making $\det(I - P(p)\Delta) = 0$:

$$\mu[N_{11}(p)] < \mu[P(p)] \tag{17}$$

This follows directly from the definition equation (15) of the structured singular value μ of a complex matrix subject to a structured Δ. As previously mentioned, $(I - N_{11}(p)\Delta)$ is expected to be nonsingular in this application, because $\mathcal{F}_u(N(p), \Delta)$ is simply a LFT representation of the bounded transfer matrix $F(p, \delta)$.

The most basic application of μ-p analysis is to visualize a set of feasible eigenvalues by evaluating $\mu(p)$ for a grid of p values in the neighborhood of a nominal eigenvalue p_0 (this is essentially what is illustrated in Fig. 1). Using a dense grid of sufficient size, it is possible, in principle, to track the eigenvalue set in the complex plane to compute the robust flutter speed and to estimate damping bounds for the mode. However, as outlined in the next section, this can be accomplished more efficiently by computing the extreme eigenvalues p_- and p_+.

In practice, the criterion equation (16) is evaluated using computable upper bounds for μ, which is in fact what guarantees robustness [18]. In the present context, this means that the regions in the complex plane in which $\mu(p) \geq 1$ will be slightly expanded, depending on the quality of the upper bound. Basically, using μ for robust flutter analysis is a sophisticated search in the parameter space for the most critical perturbation. Unfortunately, the most critical perturbation as such is not a result of the upper-bound computation, but it can be estimated by other means [9,19]. In this work, the μ solver in MATLAB [20] was used for the μ analysis, using the default settings.

Finally, it may be noted that the previous μ-k method [4–6] only considered p values along the imaginary axis, and $\mu(ik)$ was evaluated to investigate if a critical flutter eigenvalue $p = ik$ was possible for some $\Delta \in B$. The μ-k method is therefore a special case of the more versatile μ-p method.

Basic Algorithm

The μ criterion equation (16) can also be used to compute the boundary of a (distinct) eigenvalue set for a particular mode as well as the extreme eigenvalues p_- and p_+ shown in Fig. 1. The first step is to compute the nominal eigenvalue p_0. From the definition equation (15), it is clear that $\mu(p) \to \infty$ when $p \to p_0$, because the nominal eigenvalue p_0 is a solution to the uncertain flutter equation for $\Delta = 0$. Figure 1 can thus be seen as a contour plot of the positive real-valued function $\mu(p)$ at $\mu(p) = 1$, and there is a distinct peak (out of the plane) at the location of the nominal eigenvalue p_0. This is illustrated in Fig. 3, in which p_0 is understood to be located at the center of the elliptical contours. To find one point at the boundary (or contour) at which $\mu(p) = 1$, one possibility is to begin at p_0 and step in a certain direction until a value $\mu(p) < 1$ is detected. From there a bisection iteration [21] can be applied to find an accurate solution p such that $\mu(p) = 1$. Repeating this procedure for an arbitrary number of directions will allow for a visualization of the boundary, which will be illustrated in the subsequent sample test case.

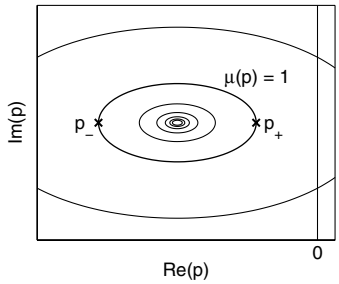

Fig. 3 Set of feasible eigenvalues as a contour plot of the $\mu(p)$ function.

Exploiting that the parameter search is embedded in the function $\mu(p)$, the eigenvalue p_+ with the maximum real part can be defined as the solution to an optimization problem with only two variables (the real and imaginary parts of p):

$$\max_p \mathrm{Re}(p) \qquad \text{subject to } \mu(p) \geq 1 \tag{18}$$

It is assumed here that the optimization is initiated at a feasible point with respect to the constraint $\mu(p) \geq 1$, such that the corresponding extreme eigenvalue is found. Hence, the optimization problem equation (18) has to be solved for each mode of interest.

In this work, a simple coordinate search was used to find the optimal solution to Eq. (18). First, a golden-section search [21] in frequency was implemented to define the function:

$$\mu_k(g) = \max_k \mu(g + ik) \tag{19}$$

This function computes the (closest) maximum value of $\mu(p)$ along a line of constant g in the complex plane as well as the maximizing frequency k^*. In the basic algorithm, the nominal frequency k_0 (the imaginary part of p_0) was used as the initial value for each golden-section search. Because the real part g^* of the extreme point p_+ satisfies $\mu_k(g^*) = 1$, upper and lower bounds for g^* were obtained by starting at the nominal value g_0 and stepping in the positive g direction until a value $\mu_k(g) < 1$ was detected. Then a bisection iteration [21] was applied to find an accurate value of g^*. Finally, the converged values of g^* and k^* were used to define the sought-for eigenvalue $p_+ = g^* + ik^*$.

The described algorithm is easy to implement and requires no derivatives of μ. As described later, the function $\mu_k(g)$ defined in Eq. (19) is also useful for model-validation purposes. The basic algorithm described previously was modified slightly to make it more efficient. For example, the golden-section search was terminated if a value $\mu(p) \geq 1$ was detected at some point, because the corresponding value of g is then known to be a lower bound of the real part of p_+. The eigenvalue p_- with the minimum real part was computed in the same manner, by performing a search in the negative g direction.

Multiple Modes

It may occur that the eigenvalue sets of different modes overlap in the complex plane in some part of the flight envelope. This situation is illustrated in Fig. 4 for two different modes at two different flight conditions. At the first flight condition (in Fig. 4a), the eigenvalue sets are distinct in the complex plane and the robust eigenvalues p_- and p_+ can be computed for both modes. However, at the second flight condition (in Fig. 4b), the eigenvalue sets overlap such that only the robust eigenvalues p_{2-} and p_{1+} can be computed.

The situation in Fig. 4b does not pose a significant problem for the robust flutter boundary because the most extreme solution (p_{1+} in the figure) can always be found, but it may obstruct the ability to find the true damping bounds for some mode in some part of the flight envelope. If this situation would be critical for some application, it is always possible to evaluate $\mu(p)$ for a grid of p values in the complex plane to investigate the complete picture in more detail. After all, this fundamental application of μ-p analysis is the main contribution of this paper.

In summary, μ-p analysis makes it possible to compute regions of feasible eigenvalues in the complex plane. From these regions, extreme eigenvalues can be extracted to estimate damping bounds and determine robust stability. These features will be exemplified in the final part of this paper.

Model Validation in the μ-p Framework

So far it has been assumed that the structure and the magnitude of the uncertainty are known. Although the structure of the uncertainty will be a result of the selection of uncertain parameters in the model, the magnitude can be more difficult to estimate. This is particularly true for aerodynamic uncertainty [4,6]. A too-low magnitude will result in a robust analysis that may not capture the worst-case perturbation, and a too-high magnitude will lead to an unnecessary conservative prediction of the robust flutter boundary.

The basic principle of model validation is to adjust the magnitude of the uncertainty to an appropriate (minimum) level by matching robust predictions against experimental data. So far, the μ framework has relied on model validation based on single-input/single-output frequency responses of the system [4,22,23]. Although this transfer-function model-validation technique can still be applied, the μ-p framework also enables model validation based on modal flight data, as described in the following sections.

Validation Based on p

Assume that a reliable estimate of an eigenvalue $p_{\mathrm{exp}} = g_{\mathrm{exp}} + ik_{\mathrm{exp}}$ has been obtained in flight testing at some given flight condition. Then the minimum magnitude of the uncertainty (in terms of the norm of the uncertainty matrix) required to make the uncertain flutter equation (2) have an eigenvalue p_{exp} is given by

$$\bar{\sigma}_p = \frac{1}{\mu(p_{\mathrm{exp}})} \tag{20}$$

where $\mu(p_{\mathrm{exp}})$ is evaluated at the same flight condition. This result follows directly from the definition of the function $\mu(p)$ in Eq. (15) and is illustrated in Fig. 5, in which $\bar{\sigma}_p$ is the minimum magnitude of the uncertainty required to expand the eigenvalue set of the particular mode to include the eigenvalue p_{exp}.

Assume, for example, that the initial uncertainty description has been scaled such that $\bar{\sigma}(\Delta) \leq 1$ corresponds to a 100% maximum variation of the uncertain parameters in the model. Then a value $\bar{\sigma}_p = 0.1$ would mean that a 10% variation is sufficient to make the

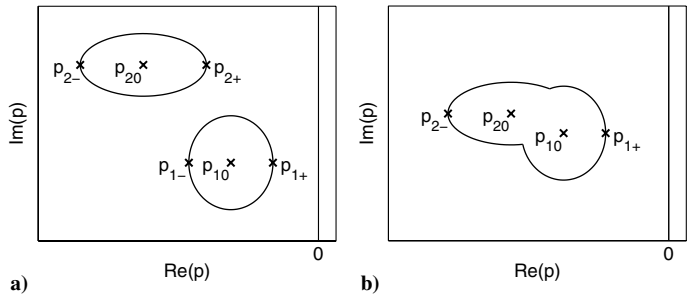

Fig. 4 Illustrations of a) distinct and b) overlapping modes in the complex plane.

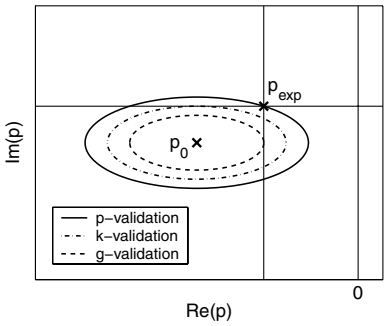

Fig. 5 Model validation in the complex plane.

uncertain flutter equation have an eigenvalue p_{exp}. This is the most basic application of the result equation (20), in which the uncertainty bounds of all parameters are scaled uniformly to validate the model (other applications are possible).

Validation Based on *g*

To avoid an excessively large uncertainty bound, in some cases it can be beneficial to validate the model against the aeroelastic damping only. This is particularly true when a discrepancy in frequency is known to be caused by a mechanism that is not captured by the uncertainty description (and has a small influence on the damping). This type of validation is referred to here as g validation.

The minimum magnitude of the uncertainty required to make an eigenvalue of the uncertain flutter equation have the real part g_{exp} can be computed as

$$\bar{\sigma}_g = \frac{1}{\mu_k(g_{\text{exp}})} \tag{21}$$

where the function $\mu_k(g)$ is defined in Eq. (19). This is also illustrated in Fig. 5, in which $\bar{\sigma}_g$ is the uncertainty bound required to expand the eigenvalue set until it touches the line $g = g_{\text{exp}}$ in the complex plane. Using this type of validation, it is thus accepted that the uncertain flutter equation does not have an eigenvalue $p = p_{\text{exp}}$, but an eigenvalue such that $\text{Re}(p) = g_{\text{exp}}$. This eigenvalue is $p = g_{\text{exp}} + ik^*$, where k^* is the frequency that maximizes $\mu(g_{\text{exp}} + ik)$.

Validation Based on *k*

By maximizing $\mu(p)$ along a line of constant frequency $k = k_{\text{exp}}$ in the complex plane, it would also be possible to perform a corresponding k validation to ensure that the flutter equation has an eigenvalue such that $\text{Im}(p) = k_{\text{exp}}$. Although validation based on frequency can be useful, p- and g-type validations are considered to be more central because of the important role played by the aeroelastic damping.

The new means for model validation introduced previously are performed on a mode-by-mode basis, meaning that an individual uncertainty bound can (in principle) be computed for each mode of interest. A major concern, however, is that the proposed technique relies on reasonably accurate frequency/damping estimation for each mode, which is typically very difficult to obtain. But if reliable data can be extracted for the most critical mode, it is then possible to isolate this mode in the model-validation procedure. The new technique also makes it possible to capture the frequency dependence of aerodynamic uncertainty in a well-defined and structured manner, by successively updating the modal uncertainty bounds in flight testing.

Application to a Wind-Tunnel Model

Although the μ-p method has already been applied to perform robust flutter analysis of the Saab JAS39 Gripen fighter aircraft [24], a more basic case study is included in this paper. The same test case was used in [4], allowing for comparison with some results obtained using the μ-k method. A 1.2 m semispan wing model with a controllable trailing-edge flap was tested in the low-speed wind tunnel L2000 at the Royal Institute of Technology, as illustrated in Fig. 6. The details of the wind-tunnel model is not accounted for here, but can be found in previous work by the author [4,25]. The model was found to suffer a 6.40 Hz flutter instability at the critical airspeed of 16.0 m/s.

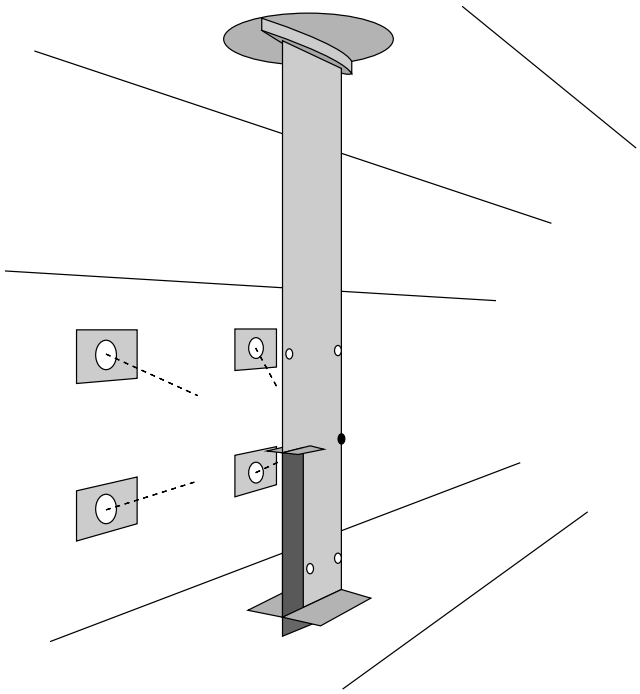

Fig. 6 Illustration of the wind-tunnel model.

Nominal Flutter Analysis

The nominal model used in [4] was obtained by combining a beam finite element model for the structural dynamics and a doublet-lattice model [26] for the unsteady aerodynamics (a standard modal formulation was used). Here, the g approximation by Chen [12] was used for the aerodynamic forces to perform analysis in the p domain. Using this model, the frequency-domain aerodynamic matrix $Q(ik)$ and its derivative $Q'(ik)$ with respect to the reduced frequency are used to obtain an aerodynamic transfer matrix $Q(p)$ that is correct to the first order in g:

$$Q(p) = Q(ik) + gQ'(ik) \tag{22}$$

This formulation is very practical because $Q(ik)$ can be computed using well-known linear aerodynamic methods [26,27]. In this work, B-splines [28] were used to obtain smooth representations of $Q(ik)$ and $Q'(ik)$ from discrete matrix data of $Q(ik)$. Further, the nominal eigenvalues were computed using a modified version of the p-k solver in [11].

Although a p-domain aerodynamic model is always desirable, the μ-p method can be applied regardless of the formulation used. If $\mu(p) \geq 1$, then p is a possible eigenvalue of the corresponding flutter equation. Consequently, robust analysis of a weakly damped mode can be performed using $Q(ik)$, if this approximation is considered to be sufficiently accurate. As the μ-p method extends standard linear flutter analysis to take uncertainty into account, the same considerations regarding modeling have to be made.

The result of the nominal flutter analysis is presented in Fig. 7 for the two most critical modes. The wing is predicted to flutter in the second mode at 14.7 m/s with a frequency of 6.43 Hz, which corresponds fairly well with the experimental flutter point. Still, the damping of the flutter mode is not fully captured by the numerical model.

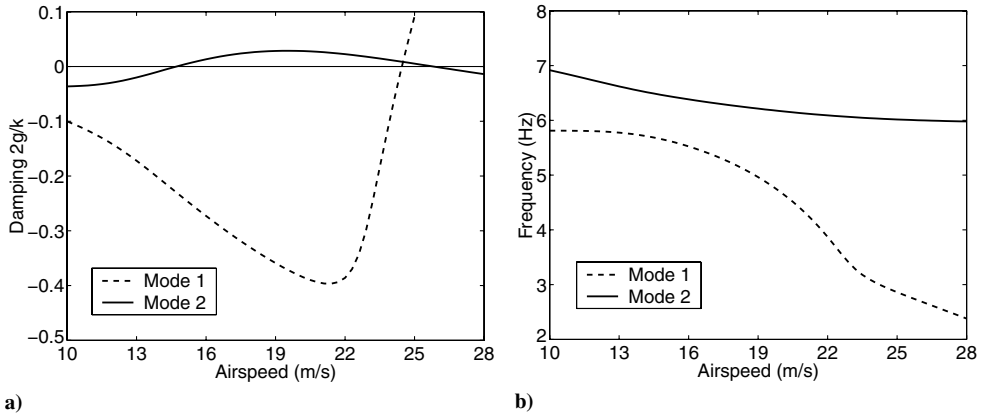

Fig. 7 Airspeed vs nominal a) damping and b) frequency.

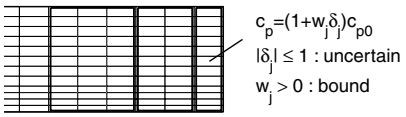

Fig. 8 Uncertain aerodynamic patches in the wing-tip region.

Uncertainty Description and LFT Formulation

In this case, the aerodynamic model is known to be incomplete, because the wing-tip plates shown in Fig. 6 are not included. Using the same technique as described in [4], an aerodynamic uncertainty description is introduced to capture their influence on the aeroelastic behavior of the wing. The aerodynamic panels in the wing-tip region are divided into three spanwise patches, as shown in Fig. 8. Within each patch, the pressure coefficients are allowed to vary in a uniform manner according to $c_p = (1 + w_j\delta_j)c_{p0}$, where c_{p0} are the nominal pressure coefficients and $w_j > 0$ is a real-valued bound such that the complex-valued uncertainty parameter δ_j satisfies $|\delta_j| \le 1$. Thus, a value of $w_j = 0.1$ means that the (complex-valued) pressure coefficients within the corresponding patch can vary up to 10%.

To pose the uncertainty description in a form suitable for μ analysis, the aerodynamic transfer matrix $Q(p)$ is partitioned according to $Q(p) = R \cdot S(p)$, where $S(p)$ computes the wing pressure coefficients from the modal deformations and R computes the modal forces from the pressure coefficients. Using the g approximation for the aerodynamic forces, the partition $S(p)$ is obtained from Eq. (22) as

$$S(p) = S(ik) + gS'(ik) \tag{23}$$

where $S(ik)$ is the corresponding partition of the computable matrix $Q(ik)$. As described in more detail in [6], the partitioned form of the aerodynamic matrix can be used to write the uncertain aerodynamic transfer matrix in the form

$$Q(p,\delta) = Q_0(p) + Q_1(p)\Delta Q_2(p) \tag{24}$$

where $Q_0(p)$ is the nominal matrix, $\Delta = \mathrm{diag}(\delta_j I_j)$ is a diagonal aerodynamic uncertainty matrix, and $Q_1(p)$ and $Q_2(p)$ are scaling matrices computed from R, $S(p)$ and the bounds w_j.

The uncertain flutter equation is obtained by inserting Eq. (24) in Eq. (1), giving

$$[F_0(p) - (\rho L^2/2)Q_1(p)\Delta Q_2(p)]\eta = 0 \tag{25}$$

where $F_0(p)$ is the nominal flutter matrix defined in Eq. (5). The LFT form Eq. (2) of the flutter equation is defined by the LFT matrix

$$N(p) = \begin{bmatrix} N_{11} & N_{12} \\ N_{21} & N_{22} \end{bmatrix} = \begin{bmatrix} 0 & Q_2 \\ -(\rho L^2/2)Q_1 & F_0 \end{bmatrix} \tag{26}$$

which provides the system matrix

$$P(p) = N_{11} - N_{12}N_{22}^{-1}N_{21} = (\rho L^2/2)Q_2F_0^{-1}Q_1 \tag{27}$$

Having derived $P(p)$ and the structure of Δ, it is now possible to perform μ-p model validation and robust analysis.

Model Validation

In the present case, only the experimental flutter point at 16.0 m/s is available for model validation, at which the critical eigenvalue is located on the imaginary axis in the complex plane. Still, this is sufficient to demonstrate μ-p model validation in practice.

The uncertainty bounds for the pressure coefficients in each patch was initially set to $w_j = 1$. Using p validation as discussed earlier, a norm $\bar{\sigma}_p = 0.17$ was required to validate the model at the experimental flutter speed (corresponding to a 17% maximum variation). The bounds were therefore updated to $w_j = 0.17$ and the boundary of the eigenvalue set was computed by finding the points at which $\mu(p) = 1$ in different directions from p_0. The resulting boundary is shown in Fig. 9 and was found to be almost circular in this case. As expected, the computed uncertainty bound expands the set to include the experimental eigenvalue. Using g validation, the uncertainty bound was reduced slightly to $\bar{\sigma}_g = 0.16$. The set is now expanded to include an eigenvalue with the same damping (real part) as the experimental eigenvalue. As can be seen in the figure, the modest reduction of the uncertainty bound using g validation is a result of the nominal and experimental eigenvalues being close in frequency.

The overall result of the model validation is that a 17% uncertainty in the spanwise load distribution is required to match the experimental flutter point. This agrees well with previous results, in which a 20% uncertainty bound was obtained using model validation based on frequency-response data [4]. However, the previous result is considered to be less reliable because it was based on an assumption about the impact of aerodynamic uncertainty in the control surface excitation.

Robust Flutter Analysis

Next, the updated model was used to perform a μ-p flutter analysis, as described previously. Nominal and robust eigenvalues

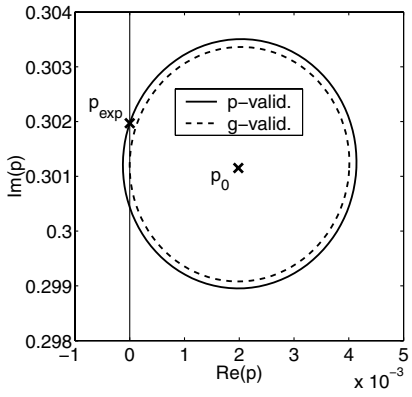

Fig. 9 Model validation at the experimental flutter speed.

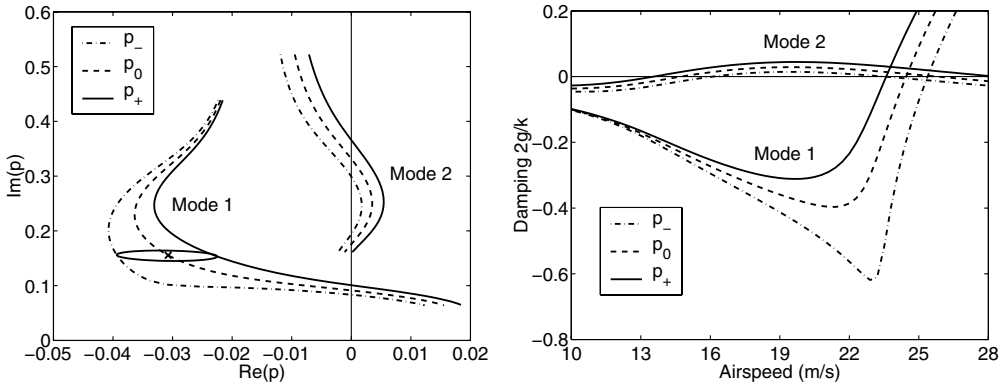

Fig. 10 Robust flutter analysis graphs for a) root locus and b) damping.

were computed for airspeeds in the range of 10 to 28 m/s. The computational effort using the μ-p method strongly depends on the dimension of the uncertainty description, but here it was comparable with that of the nominal analysis. A robust eigenvalue was thus computed in a couple of seconds. The different eigenvalues are displayed in a root-locus graph in Fig. 10a. The worst- and best-case flutter speeds for each mode are the airspeeds at which the corresponding eigenvalues p_+ and p_-, respectively, cross the imaginary axis. To give an example of how the different eigenvalues are related to each other, a set of feasible eigenvalues is shown for the first mode at 21 m/s.

The robust flutter speeds are more apparent in the damping graph in Fig. 10b. It is important to note that it is the damping $2g/k$ of the extreme eigenvalues (with minimum/maximum g) that is displayed, not the minimum/maximum values of $2g/k$. The second mode is predicted to flutter in the range of 13.6–16.2 m/s, and the first mode is predicted to flutter in the range of 23.6–25.4 m/s. Note, however, that the uncertainty bound obtained for the second mode was used for the first mode as well (because no experimental data were available for this mode). Finally, the experimental flutter speed is found to be within the predicted range of flutter speeds for the critical mode, as should be the case.

Conclusions

In this paper, it has been shown that μ analysis can be applied to perform robust eigenvalue analysis and model validation. As long as a μ upper bound of sufficient quality can be computed, μ-p analysis extends standard linear flutter analysis to take deterministic uncertainty and variation into account. Whereas a nominal method computes a single eigenvalue, the μ-p method computes a set of feasible eigenvalues. This not only allows robust analysis of the flutter speed, but also allows subcritical properties such as the frequency and damping of a particular mode. Adding the capability to perform model validation based on modal flight data, the μ-p framework has the potential to make the current procedures for flutter clearance of aircraft more reliable and efficient.

Acknowledgments

This work was financially supported by the Swedish National Aeronautics Research Program project S4303. The author is grateful to Martin Carlsson at Saab Aerosystems for the feedback that led to this development, to Ulf Ringertz for providing the spline tools used in the case study, and to Ulf Jönsson for reviewing the mathematical formulation. Finally, the author wishes to thank the reviewers for their comments and suggestions that improved the paper.

References

[1] Lind, R., and Brenner, M., *Robust Aeroservoelastic Stability Analysis*, Springer–Verlag, London, 1999.

[2] Lind, R., "Match-Point Solutions for Robust Flutter Analysis," *Journal of Aircraft*, Vol. 39, No. 1, 2002, pp. 91–99. doi:10.2514/2.2900

[3] Zhou, K., Doyle, J. C., and Glover, K., *Robust and Optimal Control*, Prentice–Hall, Upper Saddle River, NJ, 1996, Chap. 11.

[4] Borglund, D., "The μ-k Method for Robust Flutter Solutions," *Journal of Aircraft*, Vol. 41, No. 5, 2004, pp. 1209–1216. doi:10.2514/1.3062

[5] Borglund, D., "Upper-Bound Flutter Speed Estimation Using the μ-k Method," *Journal of Aircraft*, Vol. 42, No. 2, 2005, pp. 555–557. doi:10.2514/1.7586

[6] Borglund, D., and Ringertz, U., "Efficient Computation of Robust Flutter Boundaries Using the μ-k Method," *Journal of Aircraft*, Vol. 43, No. 6, 2006, pp. 1763–1769. doi:10.2514/1.20190

[7] Baldelli, D. H., Lind, R., and Brenner, M., "Robust Match-Point Solutions Using Describing Function Method," *Journal of Aircraft*, Vol. 42, No. 6, 2005, pp. 1596–1604. doi:10.2514/1.11853

[8] Moulin, B., "Modeling of Aeroservoelastic Systems with Structural and Aerodynamic Variations," *AIAA Journal*, Vol. 43, No. 12, 2005, pp. 2503–2513. doi:10.2514/1.15023

[9] Heinze, S., "Assessment of Critical Fuel Configurations Using Robust Flutter Analysis," *Journal of Aircraft*, Vol. 44, No. 6, 2007, pp. 2034–2039. doi:10.2514/1.30500

[10] Heinze, S., and Borglund, D., "Robust Flutter Analysis Considering Mode Shape Variations," *Journal of Aircraft*, Vol. 45, No. 3, 2008, pp. 1070–1074. doi:10.2514/1.28728

[11] Bäck, P., and Ringertz, U., "Convergence of Methods for Nonlinear Eigenvalue Problems," *AIAA Journal*, Vol. 35, No. 6, 1997, pp. 1084–1087. doi:10.2514/2.200

[12] Chen, P. C., "Damping Perturbation Method for Flutter Solution: The g-Method," *AIAA Journal*, Vol. 38, No. 9, 2000, pp. 1519–1524. doi:10.2514/2.1171

[13] Wilkinson, J. H., *The Algebraic Eigenvalue Problem*, Oxford Univ. Press, New York, 1965, Chap. 2.

[14] Kuttenkeuler, J., and Ringertz, U., "Aeroelastic Design Optimization with Experimental Verification," *Journal of Aircraft*, Vol. 35, No. 3, 1998, pp. 505–507. doi:10.2514/2.2330

[15] Becus, G. A., "Automated Search for the Most Critical Flutter Configuration in Models with Uncertainty," *Mathematical and Computer Modelling*, Vol. 14, 1990, pp. 977–982. doi:10.1016/0895-7177(90)90324-G

[16] Zhou, K., Doyle, J. C., and Glover, K., *Robust and Optimal Control*, Prentice–Hall, Upper Saddle River, NJ, 1996, Chap. 10.

[17] Zhou, K., Doyle, J. C., and Glover, K., *Robust and Optimal Control*, Prentice–Hall, Upper Saddle River, NJ, 1996, Chap. 2.

[18] Young, P., Newlin, M., and Doyle, J., "Practical Computation of the Mixed μ Problem," *Proceedings of the American Control Conference*, Vol. 3, Inst. of Electrical and Electronics Engineers, Piscataway, NJ, 1992, pp. 2190–2194.

[19] Hayes, M. J., Bates, D. G., and Postlethwaite, I., "New Tools for Computing Tight Bounds on the Real Structured Singular Value," *Journal of Guidance, Control, and Dynamics*, Vol. 24, No. 6, 2001,

pp. 1204–1213.
doi:10.2514/2.4836
[20] Balas, G., Chiang, R., Packard, A., and Safonov, M., *MATLAB Robust Control Toolbox User's Guide*, Release 2007a, The MathWorks, Inc., Natick, MA, 2007.
[21] Gill, P. E., Murray, W., and Wright, M. H., *Practical Optimization*, Academic Press, London, 1981.
[22] Kumar, A., and Balas, G. J., "An Approach to Model Validation in the μ Framework," *Proceedings of the American Control Conference*, Inst. of Electrical and Electronics Engineers, Piscataway, NJ, 1994, pp. 3021–3026.
[23] Brenner, M., "Aeroservoelastic Model Uncertainty Bound Estimation from Flight Data," *Journal of Guidance, Control, and Dynamics*, Vol. 25, No. 4, 2002, pp. 748–754.
[24] Carlsson, M., and Karlsson, A., "Robust Aeroelastic Analysis of the Gripen Fighter Including Flight Test Model Validation," CEAS/AIAA/KTH International Forum on Aeroelasticity and Structural Dynamics (IFASD 2007), Royal Inst. of Technology Paper IF-019, Stockholm, Sweden, June 2007.
[25] Borglund, D., and Kuttenkeuler, J., "Active Wing Flutter Suppression Using a Trailing Edge Flap," *Journal of Fluids and Structures*, Vol. 16, No. 3, 2002, pp. 271–294.
doi:10.1006/jfls.2001.0426
[26] Albano, E., and Rodden, W. P., "A Doublet-Lattice Method for Calculating Lift Distributions on Oscillating Surfaces in Subsonic Flows," *AIAA Journal*, Vol. 7, No. 2, 1969, pp. 279–285.
doi:10.2514/3.5086
[27] Chen, P. C., Lee, H. W., and Liu, D. D., "Unsteady Subsonic Aerodynamics for Bodies and Wings with External Stores Including Wake Effect," *Journal of Aircraft*, Vol. 30, No. 5, 1993, pp. 618–628.
doi:10.2514/3.46390
[28] De Boor, C., *A Practical Guide to Splines*, Springer–Verlag, New York, 2001, Chap. 9.

J. Cooper
Associate Editor